

Magic Doping Fractions in High-Temperature Superconductors

Seiki Komiya,¹ Han-Dong Chen,² Shou-Cheng Zhang,² and Yoichi Ando¹

¹*Central Research Institute of Electric Power Industry, Komae, Tokyo 201-8511, Japan*

²*Department of Physics, McCullough building, Stanford University, Stanford, CA 94305*

We report hole-doping dependence of the in-plane resistivity ρ_{ab} in a cuprate superconductor $\text{La}_{2-x}\text{Sr}_x\text{CuO}_4$, carefully examined using a series of high-quality single crystals. Our detailed measurements find a tendency towards charge ordering at particular rational hole doping fractions of $1/16$, $3/32$, $1/8$, and $3/16$. This observation appears to suggest a specific form of charge order and is most consistent with the recent theoretical prediction of the checkerboard-type ordering of the Cooper pairs at rational doping fractions $x = (2m + 1)/2^n$, with integers m and n .

PACS numbers: 74.25.Fy, 74.25.Jb, 74.25.Dw, 74.72.Dn

All high- T_c cuprates contain three robust phases — the insulating antiferromagnetic (AF) phase, the superconducting (SC) phase, and the metallic phase — depending on the density of charge carriers introduced by doping. However, in some cuprate materials, there are also other electronic phases which compete with superconductivity [1, 2]. Determining the nature of these competing phases is a key focus of the current research in high-temperature superconductivity. One particularly important type of competing phase is a charge-ordered phase in underdoped cuprates, where the carrier density is smaller than the optimum level for superconductivity. In the underdoped regime, the mean kinetic energy of the carriers is low because of the small carrier density, and the Coulomb interaction plays an important role. The Coulomb interaction generally prefers some form of charge order, whose detailed form could be affected by the local antiferromagnetic exchange energy as well. One possibility is that the charges form one-dimensional (1D) stripes [2, 3, 4, 5, 6]. Experimentally, magnetic and lattice neutron scattering on $\text{La}_{2-x}\text{Sr}_x\text{CuO}_4$ (LSCO) and its family compounds has been interpreted in terms of the 1D stripe picture [2, 7], although the two-dimensional (2D) nature of the spin system has recently been emphasized in Refs. [8, 9]. Considering the presence of strong pairing interactions in this material, Chen *et al.* [10, 11, 12] have proposed a 2D checkerboard-type ordering of the hole pairs. It offers a natural explanation of the scanning tunneling microscopy (STM) results on $\text{Bi}_2\text{Sr}_2\text{CaCu}_2\text{O}_{8+\delta}$ (BSCCO) and $\text{Ca}_{2-x}\text{Na}_x\text{CuO}_2\text{Cl}_2$ (NCCOC) compounds, which show rotationally symmetric $4a \times 4a$ charge ordering patterns [13, 14, 15, 16, 17]. The checkerboard state of the Cooper pairs has also been discussed in other frameworks in the recent literature [18, 19, 20, 21]. Furthermore, the possibility of a Wigner crystal of single holes has also been proposed as a competing charge ordered state at low doping [22, 23, 24]. In view of the contrasting experimental results and theoretical proposals, more systematic studies of the nature of the charge order in the cuprates are clearly called for.

The charge ordering tendency is expected to be particularly pronounced near certain “magic” doping lev-

els, where the charge modulation is commensurate with the underlying lattice [11, 20, 21, 22]. Motivated by the recent discussions on the stripe versus the checkerboard order, we carry out a systematic study of the doping dependence of the resistivity, in order to uncover the possible commensurability effects. Thanks to the greatly improved crystal-growth technique for LSCO using floating-zone furnaces, single crystals of LSCO of unprecedented quality have recently become available [25] for a very wide doping range. The cleanliness of the new-generation crystals has allowed, for example, to produce 100%-untwinned single crystals [26], which in turn led to finding of novel physics in this system [27, 28, 29]. In this work, we systematically measure the temperature dependence of the in-plane resistivity ρ_{ab} in a series of high-quality LSCO crystals for $x = 0.009 - 0.216$. The raw data of $\rho_{ab}(T)$ are shown in Fig. 1 for all the superconducting samples; note that the hole doping is changed in very small increments (typically 1%) here, which is necessary for analyzing how exactly the mobility of the holes changes with their density.

Figure 2(a) shows the x dependence of the inverse mobility μ^{-1} , which is equal to $n e \rho_{ab}$, for representative temperatures (the hole density n is given by x/V , where V is the unit volume per Cu). Also, since the absolute values of μ^{-1} are subject to possible geometrical-factor errors (which can be up to 5% in the case of our measurements), in Fig. 2(b) we show $\rho_{ab}(T)/\rho_{ab}(300\text{K})$, which factors out such geometrical-factor errors. One can easily see that at high temperature the x dependencies of these variables are rather smooth and featureless, but with lowering temperature they start to “oscillate”; a peak at $x \simeq 0.13$ is particularly evident. In addition, there are three more peaks and/or shoulders, if weaker, at $x \simeq 0.06$, 0.09 , and 0.18 . This observation suggests that there are particular carrier densities where the hole motion tends to be hindered, which weakly enhances the resistivity at low temperature. Most naturally, such a behavior is indicative of a “commensurability” effect associated with some sort of charge ordering [11, 20, 21, 22]. Remember, in usual charge ordered systems where the Peierls transition is responsible, a sharp increase in resistivity is

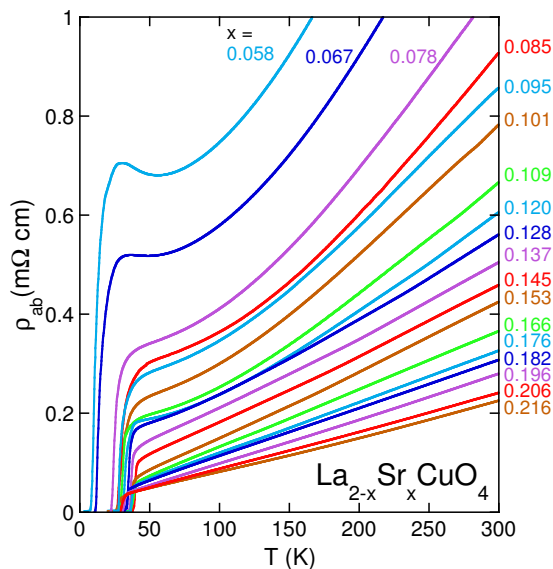


FIG. 1: Temperature dependences of ρ_{ab} for a series of LSCO single crystals. The x values shown are the actual Sr contents measured by the inductively-coupled-plasma atomic-emission spectroscopy (ICP-AES). The samples are carefully annealed to remove excess oxygens or oxygen vacancies, so the hole density in the present samples are essentially equal to x .

observed upon charge ordering [30]; in the present case, where the Coulomb interaction is likely to be responsible, the effect appears to be milder. The observed decimal numbers (0.06, 0.09, 0.13 and 0.18) suggest that the commensurability effect is possibly taking place at rational doping levels $1/16$, $3/32$, $1/8$, and $3/16$. (We note that there has been some preliminary evidence for a charge ordering tendency at $x = 1/16$ [23, 24]).

Given that the inverse mobility shows an x -dependence that is indicative of charge ordering, one may wonder how the superconducting transition temperature T_c changes with x ; the inset of Fig. 2(a) shows the x -dependence of the zero-resistivity T_c in our series of samples. Besides a plateau-like feature for $x = 0.08 - 0.12$, the T_c changes rather smoothly without showing clear dips that can be associated with the magic fractions observed in the resistivity data. Hence, the putative charge order appears to be *not* particularly destructive to superconductivity; this is rather surprising, but is probably related to the STM observation [15] that the checkerboard order shows up as a *precursor* to superconductivity. In this regard, it is useful to note that most of the other experiments concerning the checkerboard state were done below T_c [13, 14, 16, 17], while the existence of the magic doping fractions is suggested in the resistivity data above T_c ; if the charge ordering phenomena in cuprates involve the Cooper pairs [11, 18, 19, 20, 21] and those pairs are formed at $T > T_c$, it is possible that the charge ordering, observable when the superconductivity is weakened, is essentially of the same nature across T_c .

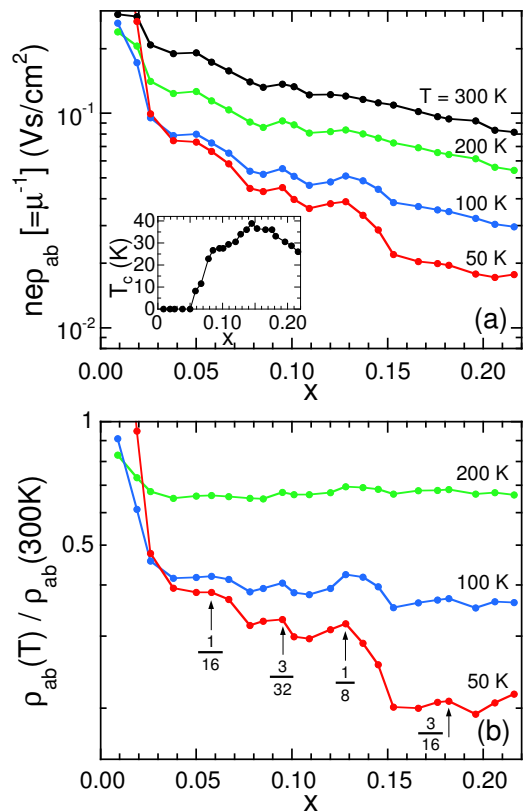


FIG. 2: (a) x -dependence of the inverse mobility μ^{-1} ($= ne\rho_{ab}$) at representative temperatures. Inset shows the x -dependence of zero-resistivity T_c . (b) x -dependence of $\rho_{ab}(T)/\rho_{ab}(300\text{K})$ at $T = 200, 100,$ and 50 K. The hole motion tends to be hindered at low temperature at $x \simeq 0.06, 0.09, 0.13,$ and 0.18 , which corresponds to the “magic” doping fractions of $1/16, 3/32, 2/16,$ and $3/16$.

Now let us discuss the theoretical implications of our data. The 1D stripe model predicts a particular set of “magic” doping fractions. The stripe model most often discussed in the literature involves site-centered, horizontal or vertical charge stripes separated by the AF domains at a commensurate distance of $d = pa$, where p is an integer and a is the lattice constant. (For the case of $p = 4$, see, for example, Fig. 1 of Ref. [7]). The holes fill alternating sites on the charge stripe. In the stripe literature, it is commonly assumed that the hole doping on the stripe stays fixed, while the inter-stripe separation varies to accommodate different values of the doping level. This simple picture predicts magic doping fractions of $x = 1/2p$, with a charge unit-cell of $2a \times pa$.

On the other hand, the 2D checkerboard-type order generally leads to a different set of magic doping fractions. Stimulated by the checkerboard orders observed by STM [13, 14, 15, 16, 17], a global phase diagram of cuprate superconductors has been theoretically proposed and numerically analyzed [10, 11, 12], where the zero-temperature phase diagram was examined in the two-

dimensional parameter space of chemical potential versus the ratio of the hole kinetic energy over the Coulomb interaction, within the framework of the $SO(5)$ theory. Most intriguingly, this theory predicts, besides the AF and SC states, checkerboard-type ordering of the Cooper pairs at magic rational doping fractions $(2m+1)/2^n$, where m and n are integers [11]. A hierarchy construction of the checkerboard states is shown in Fig. 3. The energetics of the checkerboard state has been studied extensively in Ref. [12], both numerically and analytically. In general, at the magic doping fraction $x = (2m+1)/2^n$, the charge unit-cell is $2^{(n+1)/2}a \times 2^{(n+1)/2}a$, pointing along the original Cu-O bond direction when n is odd, and along the diagonal direction when n is even. This theory relies on mapping the original fermionic degrees of freedom into effective bosonic degrees of freedom [11]; such mapping may be justified in the underdoped and optimally doped regimes, but fails in heavily doped samples. Therefore, while the bosonic theory predicts all magic doping fractions at $x = (2m+1)/2^n$, one can only expect the effective theory to be valid for $x < 1/4 = 25\%$. Also, it is generally expected that the charge ordering tendencies are stronger at higher levels of the hierarchy, with smaller n .

Both the 1D stripe model and the 2D checkerboard model adequately explain the dominant magic doping fraction at $x = 1/8$, but they predict different sets of magic doping fractions, at which the system is expected to develop charge ordering tendencies. In this regard, our extensive data set on the doping dependence, if it indeed reflects a charge ordering tendency, contains sufficient accuracy to distinguish between the simple 1D stripe model and the 2D checkerboard model discussed above. The simple stripe model predicts commensurate effect at magic doping fractions $1/4, 1/6, 1/8, 1/10, 1/12, 1/14, 1/16$, which should be either equally strong or vary monotonically in strength; therefore, the absence of any commensurability effects at $x = 1/6$ and $x = 1/10$ in our data or any other previous experiments is puzzling in the simple stripe model. Although the stripe structure can yield a complex “devil’s staircase” of commensurate dopings in nickelates [31], the magic fractions suggested here in a cuprate superconductor would be a challenge to the stripe picture. On the other hand, the suggested series ($1/16, 3/32, 1/8, \text{ and } 3/16$) agrees surprisingly well with the magic doping fractions predicted from the checkerboard model discussed above, up to the level $n = 5$. At this level, the absence of the $1/32$ fraction is understandable, since the hole-pair lattice at this doping fraction would be very dilute and therefore disordered. More notable is the absence of the $5/32$ fraction, for which we do not have an adequate explanation at this moment. In passing, let us briefly mention the Wigner crystal of single holes, which has the charge unit-cell $2^{n/2}a \times 2^{n/2}a$ at $x = 1/2^n$. The main difference between the pair checkerboard and the hole checkerboard is not only the size of

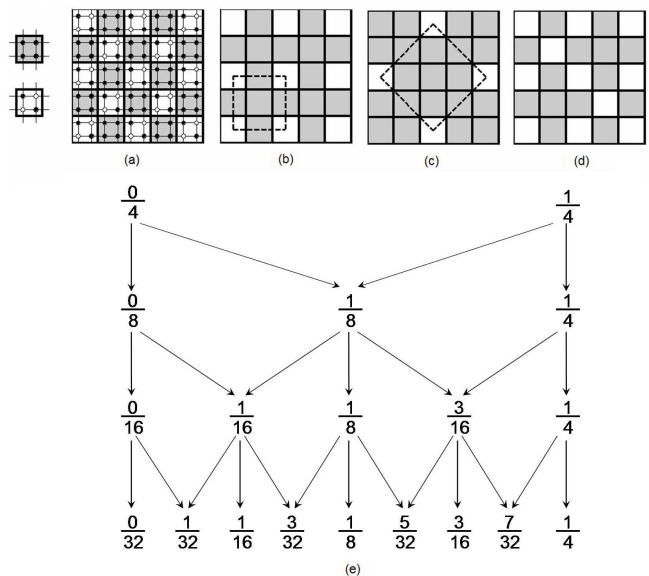


FIG. 3: Hierarchical construction of the checkerboard-type ordering of the hole pairs at “magic” doping fractions $(2m+1)/2^n$, where m and n are integers. Following the construction of Ref. [11], the original CuO_2 lattice is grouped into non-overlapping plaquettes, which can be represented by the squares on a checkerboard. A checkerboard can be alternately colored black and white; in our case, each black square contains four sites and no holes, while each white square contains four sites and two holes in the form of a Cooper pair. Such a state has hole doping density $x = 1/4$ (a), as represented at the highest level of the hierarchy (e). (Electrons are denoted by black dots, and holes are denoted by open dots; since we only address the issue of charge ordering here, the spin of the electron is not explicitly indicated). At the next level of the hierarchy, consider the lattice of white squares only, and alternately color half of them black. Such a state has hole doping density $x = 1/8$ (b). At one further level down in the hierarchy, one can either consider the lattice of the white squares, and alternately color half of them black, thus obtaining a state with $x = 1/16$ (c), or one can consider the lattice of the newly colored black squares and alternately color half of them white, thus obtaining a state with $x = 3/16$ (d). This hierarchy construction can be obviously iterated *ad infinitum*, generating a binary tree of magic doping fractions as shown here in (e).

the charge unit-cell but also their orientations, which are 45° with respect to each other; thus, the two should be easily discernible in experiments at a given doping.

Neutron scattering on the LSCO-based materials have provided an extensive set of data on the *spin* order. We note, however, that the nature of the spin order may not be directly related to the nature of the charge order reflected in the transport properties, particularly in the superconducting doping regime of LSCO where the spin order is mostly dynamic [32]. If the magnetic incommensurability observed by the neutron scattering is part of some dynamic dispersing mode [8, 9, 33], it is natural that the incommensurability does not represent

the unit-cell of the incipient charge order. Furthermore, at $x = 0.02$, the magnetic neutron scattering found static and unidirectional spin stripes that are no less than 30 unit-cell apart (magnetic incommensurability δ is 0.016) [34], which would cause a large resistivity anisotropy if the charges are conforming to the 1D spin stripes. However, transport measurements on untwinned single crystals have found only a factor of 1.5 resistivity anisotropy between the “longitudinal” and “transverse” directions [27]; this is rather difficult to understand without invoking some 2D character (which can, for example, be coming from a nematic stripe order [35]) in the charge system. In passing, we note that our transport measurements of LSCO have found evidence for charge self-organization [36, 37] and modest one-dimensionality [27, 28] only in the lightly doped regime ($x \leq 0.05$) of this compound, while the present study suggests the existence of the checkerboard order only in the superconducting doping regime ($x \geq 0.06$). We also note that the measurements of the in-plane resistivity anisotropy become impractical for $x \geq 0.06$, because the structural transition temperature (below which the system becomes orthorhombic) comes close to or below the room temperature at these dopings, making it difficult to prepare untwinned samples.

There are only a few direct experimental observations of charge order in the LSCO-based materials. Neutron scattering on the $\text{La}_{1.48}\text{Nd}_{0.4}\text{Sr}_{0.12}\text{CuO}_4$ (LNSCO) compound at $x = 1/8$ reveals elastic charge order peaks [38] which can be interpreted either as orthogonally intersecting stripes on alternating planes or in the same plane. The latter case would also be consistent with the 2D pair checkerboard pattern with the charge unit-cell $4a \times 4a$. While it is fair to mention that the details of the charge order in LNSCO are more consistent with the 1D stripe picture [39], such a structure may well be a result of the 1D modulation arising from the explicit symmetry breaking in the low-temperature tetragonal (LTT) phase of this particular material, and therefore may not be representative of the charge order in Nd-free LSCO.

In view of the intriguing agreement of the present transport data with the hole pair checkerboard model, it would be desirable to systematically perform direct measurements of the charge order in the LSCO-based materials by some means. If the proposed checkerboard states are indeed realized in LSCO, the orientation of the charge unit cell should be along the Cu-O bond direction at $x = 1/8$ (as is the case in BSCCO or NCCOC), while it should be along the diagonal direction near $x = 1/16$; it would be definitive if this rotation of the charge unit cell upon changing x is confirmed by a direct means. Also, since some fractions suggested in the present measurements are relatively weak, it would be highly desirable to carry out these systematic transport measurements under high magnetic fields or under high pressure, where one would expect the competing order to be enhanced

and the magic doping fractions to be more pronounced.

We would like to thank P. W. Anderson, S. A. Kivelson, J. M. Tranquada, A. Yazdani and Z. X. Zhao for helpful discussions. This work is supported by the Grant-in-Aid for Science provided by the Japanese Society for the Promotion of Science, the NSF under grant numbers DMR-0342832, and the US Department of Energy, Office of Basic Energy Sciences, under contract DE-AC03-76SF00515.

-
- [1] S. Sachdev and S.-C. Zhang, *Science* **295**, 452 (2002).
 - [2] S. A. Kivelson, I. P. Bindloss, E. Fradkin, V. Oganesyan, J. M. Tranquada, A. Kapitulnik, and C. Howald, *Rev. Mod. Phys.* **75**, 1201 (2003).
 - [3] J. Zaanen and O. Gunnarsson, *Phys. Rev. B* **40**, R7391 (1989).
 - [4] M. Kato, K. Machida, H. Nakanishi, and M. Fujita, **59**, 1047 (1990).
 - [5] S. R. White and D. J. Scalapino, *Phys. Rev. Lett.* **80**, 1272 (1998).
 - [6] M. Vojta and S. Sachdev, *Phys. Rev. Lett.* **83**, 3916 (1999).
 - [7] J. M. Tranquada, B. J. Sternlieb, J. D. Axe, Y. Nakamura, and S. Uchida, *Nature* **375**, 561 (1995).
 - [8] N. B. Christensen, D. F. McMorrow, H. M. Ronnow, B. Lake, S. M. Hayden, G. Aeppli, T. G. Perring, M. Mangkorntong, M. Nohara, and H. Tagaki, *Phys. Rev. Lett.* **93**, 147002 (2004).
 - [9] S. M. Hayden, H. A. Mook, P. Dai, T. G. Perring, and F. Dogan, *Nature (London)* **429**, 531 (2004).
 - [10] H. D. Chen, J. P. Hu, S. Capponi, E. Arrighoni, and S. C. Zhang, *Phys. Rev. Lett.* **89**, 137004 (2002).
 - [11] H.-D. Chen, S. Capponi, F. Alet, and S.-C. Zhang, *Phys. Rev. B* **70**, 024516 (2004).
 - [12] H.-D. Chen, O. Vafek, A. Yazdani, and S.-C. Zhang, *Phys. Rev. Lett.* **93**, 187002 (2004).
 - [13] J. E. Hoffman, E. W. Hudson, K. M. Lang, V. Madhavan, H. Eisaki, S. Uchida, and J. C. Davis, *Science* **295**, 466 (2002).
 - [14] C. Howald, H. Eisaki, N. Kaneko, M. Greven, and A. Kapitulnik, *Phys. Rev. B* **67**, 014533 (2003).
 - [15] M. Vershinin, S. Misra, S. Ono, Y. Abe, Y. Ando, and A. Yazdani, *Science* **303**, 1995 (2004).
 - [16] K. McElroy, D.-H. Lee, J. E. Hoffman, K. M. Lang, E. W. Hudson, H. Eisaki, S. Uchida, J. Lee, and J. Davis, *cond-mat/0404005*.
 - [17] T. Hanaguri, C. Lupien, Y. Kohsaka, D.-H. Lee, M. Azuma, M. Takano, H. Takagi, and J. C. Davis, *Nature (London)* **430**, 1001 (2004).
 - [18] E. Altman and A. Auerbach, *Phys. Rev. B* **65**, 104508 (2002).
 - [19] M. Vojta, *Physical Review B* **66**, 104505 (2002).
 - [20] Z. Tesanovic, *Phys. Rev. Lett.* **93**, 217004 (2004).
 - [21] P. W. Anderson, *cond-mat/0406038*.
 - [22] H. C. Fu, J. C. Davis, and D.-H. Lee, *cond-mat/0403001*.
 - [23] Y. H. Kim and P. H. Hor, *Mod. Phys. Lett. B* **15**, 497 (2001).
 - [24] F. Zhou, P. H. Hor, X. L. Dong, W. X. Ti, J. W. Xiong, and Z. X. Zhao, *Physica C* **408–410**, 430 (2004).

- [25] S. Komiya, Y. Ando, X. F. Sun, and A. N. Lavrov, Phys. Rev. B **65**, 214535 (2002).
- [26] A. N. Lavrov, Y. Ando, S. Komiya, and I. Tsukada, Phys. Rev. Lett. **87**, 017007 (2001).
- [27] Y. Ando, K. Segawa, S. Komiya, and A. N. Lavrov, Phys. Rev. Lett. **88**, 137005 (2002).
- [28] M. Dumm, S. Komiya, , Y. Ando, and D. N. Basov, Phys. Rev. Lett. **91**, 077004 (2003).
- [29] A. N. Lavrov, S. Komiya, and Y. Ando, Nature **418**, 385 (2002).
- [30] G. Grüner, Rev. Mod. Phys. **60**, 1129 (1988).
- [31] P. Wochner, J. M. Tranquada, D. J. Buttrey, and V. Sachan, Phys. Rev. B **57**, 1066 (1998).
- [32] K. Yamada, C. H. Lee, K. Kurahashi, J. Wada, S. Wakimoto, S. Ueki, H. Kimura, Y. Endoh, S. Hosoya, G. Shirane, et al., Physical Review B **57**, 6165 (1998).
- [33] M. R. Norman, Phys. Rev. B **61**, 14751 (2000).
- [34] M. Matsuda, M. Fujita, K. Yamada, R. J. Birgeneau, M. A. Kastner, H. Hiraka, Y. Endoh, S. Wakimoto, and G. Shirane, Physical Review B **62**, 9148 (2000).
- [35] S. A. Kivelson, E. Fradkin, and V. J. Emery, Nature (London) **393**, 550 (1998).
- [36] Y. Ando, A. N. Lavrov, S. Komiya, K. Segawa, and X. F. Sun, Phys. Rev. Lett. **87**, 017001 (2001).
- [37] Y. Ando, A. N. Lavrov, and S. Komiya, Phys. Rev. Lett. **90**, 247003 (2003).
- [38] J. M. Tranquada, J. D. Axe, N. Ichikawa, Y. Nakamura, S. Uchida, and B. Nachumi, Phys. Rev. B **54**, 7489 (1996).
- [39] M. v. Zimmermann et al., Europhys. Lett. **41**, 629 (1998).